^{18}F-choline in experimental soft tissue infection assessed with autoradiography and high-resolution PET

Matthias T. Wyss[1, 2], Bruno Weber[1], Michael Honer[2], Nicolas Späth[1], Simon M. Ametamey[2], Gerrit Westera[2], Beata Bode[4], Achim H. Kaim[3], Alfred Buck[1]

[1] PET Center, Division of Nuclear Medicine, University Hospital Zurich, Zurich, Switzerland
[2] Center for Radiopharmaceutical Science of ETH, PSI and USZ, Paul Scherrer Institute, Villigen, Switzerland
[3] Klinik Im Schachen, Aarau, Switzerland
[4] Institute of Pathology, University Hospital, Zurich, Switzerland

Received: 3 June 2003 / Accepted: 27 July 2003 / Published online: 20 November 2003

Abstract. For each oncological tracer it is important to know the uptake in non-tumorous lesions. The purpose of this study was to measure the accumulation of fluorine-18 choline (FCH), a promising agent for the evaluation of certain tumour types, in infectious tissue. Unilateral thigh muscle abscesses were induced in five rats by intramuscular injection of 0.1 ml of a bacterial suspension (*Staphylococcus aureus*, 1.2×10^9 CFU/ml). In all animals, FCH accumulation was measured with high-resolution positron emission tomography (PET) on day 6. Autoradiography of the abscess and ipsilateral healthy muscle was performed on day 7 (three animals) and day 11 (two animals) and correlated with histology. In addition, ^{18}F-fluorodeoxyglucose (FDG) PET was performed on day 5. Increased FCH uptake was noted in specific layers of the abscess wall which contained an infiltrate of mainly granulocytes on day 7 and mainly macrophages on day 11. The autoradiographic standardised uptake values in the most active part of the abscess wall were 2.99 on day 7 (n=3) and 4.05 on day 11 (n=2). In healthy muscle the corresponding values were 0.99 and 0.64. The abscesses were clearly visualised on the FCH and FDG PET images. In conclusion, this study demonstrated avid FCH accumulation in inflammatory tissue, which limits the specificity of FCH for tumour detection. Future studies are now needed to determine the degree of this limitation in human cancer patients.

Keywords: Soft tissue infection – ^{18}F-choline – ^{18}F-fluorodeoxyglucose – Autoradiography – PET – Tumour imaging

Alfred Buck (✉)
PET Center, Division of Nuclear Medicine,
University Hospital Zurich, Rämistrasse 100,
8091 Zurich, Switzerland
e-mail: buck@nuklearmed.unizh.ch
Tel.: +41-1-2553547, Fax: +41-1-2554414

Eur J Nucl Med Mol Imaging (2004) 31:312–316
DOI 10.1007/s00259-003-1337-4

Introduction

Whole-body positron emission tomography (PET) has developed into an invaluable tool for the evaluation of tumours. By far the largest number of examinations are performed with fluorine-18 fluorodeoxyglucose (FDG). However, FDG has several disadvantages. One is the reduced specificity for tumour cells due to FDG uptake in inflammatory lesions. A promising candidate for higher tumour specificity was ^{18}F-ethyl tyrosine (FET), which does not accumulate in inflammatory lesions [1] and which had shown promising potential in the evaluation of brain tumour patients [2]. Unfortunately, FET proved to be less sensitive than FDG in whole-body imaging of certain tumours [3]. Another substantial disadvantage of FDG is the minimal or lacking uptake in certain tumours, such as prostate carcinoma, the most common cancer in elderly men. Promising results for staging patients with prostate carcinoma have been reported with labelled choline compounds. Some studies have used carbon-11 labelled choline [4, 5, 6], whose clinical usefulness is limited by the short half-life of ^{11}C. This problem is overcome by ^{18}F-labelled choline (FCH), which has recently been introduced and has also shown promising results in the evaluation of patients with prostate cancer [7, 8, 9, 10]. For every tumour imaging compound it is important to know the accumulation characteristics in non-tumorous lesions, of which inflammatory/infectious foci are among the most important. Thus, the purpose of this study was to assess the FCH uptake in infected tissue. As in our previous studies, we used a rat model with experimentally induced abscesses in a leg muscle [1, 10]. FCH accumulation was determined using high-resolution PET

and autoradiography. In addition, FDG PET was performed in each animal.

Materials and methods

Animals and abscess model. This study was performed according to the guidelines of the National Institutes of Health and the recommendations of the committee on animal research at our institution. The protocol was approved by the local institutional review committee on animal care.

The study included five Sprague-Dawley rats (weight 250–300 g). All the animals were kept in cages with standardised conditions of light and free access to water and food. Using general inhalation anaesthesia (isoflurane, Forene, Abbott Laboratories), a unilateral deep calf muscle abscess was induced by intra muscular inoculation (25G needle) of 0.1 ml of a bacterial suspension (*Staphylococcus aureus*, clinical strain 10B, Novartis Pharma, Inc., Switzerland). The bacterial concentration (1.2109 CFU/ml) was measured by optical density (McFarland Standard, bioMerieux, Inc., USA).

All animals developed a palpable fluctuating mass in the left calf muscle within 36 h after bacterial inoculation. No systemic infection occurred.

Positron emission tomography with FCH and FDG. Examination were performed on a high-resolution PET system (16 Module quad Hidac PET System). The resolution at the centre of the field of view was 1.0 mm. FDG PET was performed 5 days after the induction of the abscess. Twenty minutes of data were acquired in list mode starting 40 min following the injection of 10–19 MBq FDG into the tail vein. FCH PET was performed 1 day later. Forty-five minutes of data were acquired immediately following injection of 8–20 MBq FCH into the tail vein. The list mode data were then rebinned into nine frames of 5 min duration. Injection and imaging with both tracers were done under isoflurane inhalation anaesthesia. To quantify tracer uptake a 10-ml syringe filled with an ^{18}F solution of known concentration (0.5–1.5 MBq/ml) was imaged immediately following the animal examination. The raw data were reconstructed using the iterative one pass list-mode–expectation maximisation (OPL-EM) algorithm (0.5 mm bin size, 200×200×440 matrix size) incorporating resolution recovery. Volumes of interest (VOIs) were subsequently placed on various tissue areas using the software PMOD [11]. The uptake values were expressed in kBq/ml using the syringe calibration. Dividing the tissue uptake by the injected activity per gram of body weight yielded the standardised uptake value (SUV).

Autoradiography with FCH. Autoradiography was performed 7 days (three animals) and 11 days (two animals) following induction of the abscess. For injection of the radiotracer a catheter was put into the right femoral vein under isoflurane anaesthesia. Ten minutes following the injection of 100–200 MBq FCH, the animals were sacrificed by an intravenous overdose of pentobarbital. Infected calf muscle and ipsilateral normal calf muscle were dissected immediately and frozen in isopentane cooled to −50°C. The frozen samples were cut (10 µm thickness) and thaw-mounted on glass slides. The slides were then put on a phosphor imager screen (Fuji TR 2025) for 4 h together with ^{14}C standards for quantification of tracer uptake. The data were scanned (Fuji BAS 1800 II, pixel size 50 µm) and converted to kBq/mg. For histological examination the slices were stained using haematoxylin-eosin (H-E).

Quantitative analysis. In a previous calibration experiment, each ^{14}C standard was assigned a value in kBq/ml of ^{18}F activity. For this purpose, 10-µm-thick slices of tissue homogenate that contained defined amounts of ^{18}F activity (kBq/mg) were exposed on the phosphor imaging screen together with the ^{14}C standard for 4 h. Using this calibration allowed conversion of the gray values into absolute uptake values (kBq/ml) at the beginning of screen exposure. To calculate standardised uptake values (SUVs) the injected activity was also decay-corrected to the same time point. The SUVs were then obtained by dividing the tissue uptake by the injected activity per gram of body weight. Regions of interest were subsequently placed on several tissue areas using the software PMOD [11].

Histology. After the autoradiographic measurements with the phosphor imaging system, the same slices were stained with H-E for histological examination.

Results

Histomorphological correlation to FCH autoradiography

A typical autoradiograph of an abscess formation on day 7 is shown together with the histology in Fig. 1. The acute abscess formation is histologically characterised by central necrosis surrounded by a layer consisting mostly of necrotic granulocytes. Adjacent to this layer is a zone of granulation tissue with an active inner part and a more mature outer part. The inner layer contains granulocytes, macrophages, myofibroblasts, blood capillaries and bacteria. The outer part is composed of the same elements but contains fewer inflammatory cells (granulocytes and macrophages) and more mature collagen. Superposition of the histological and autoradiographic image of the identical slice clearly demonstrated that the highest FCH concentration was in layer 3; no FCH at all was noted in layer 2. On day 11, layer 2 was even more necrotic and granulocytes were no longer present in layers 3 and 4.

The SUVs (mean) of layers 3 and 4 are summarised in Table 1. In the three animals examined 7 days and the

Table 1. FCH SUV determined by autoradiography

Animal	Day[a]	Abscess wall[b]		Muscle SUV
		Inner	Outer	
1	7	2.96	2.13	0.85
2	7	2.94	2.02	0.95
3	7	3.07	2.12	1.16
4	11	4.02	2.82	0.61
5	11	4.07	2.95	0.67

[a] Day of autoradiography following induction of abscess
[b] Inner: layer 3 in Fig. 1; outer: layer 4 in Fig. 1

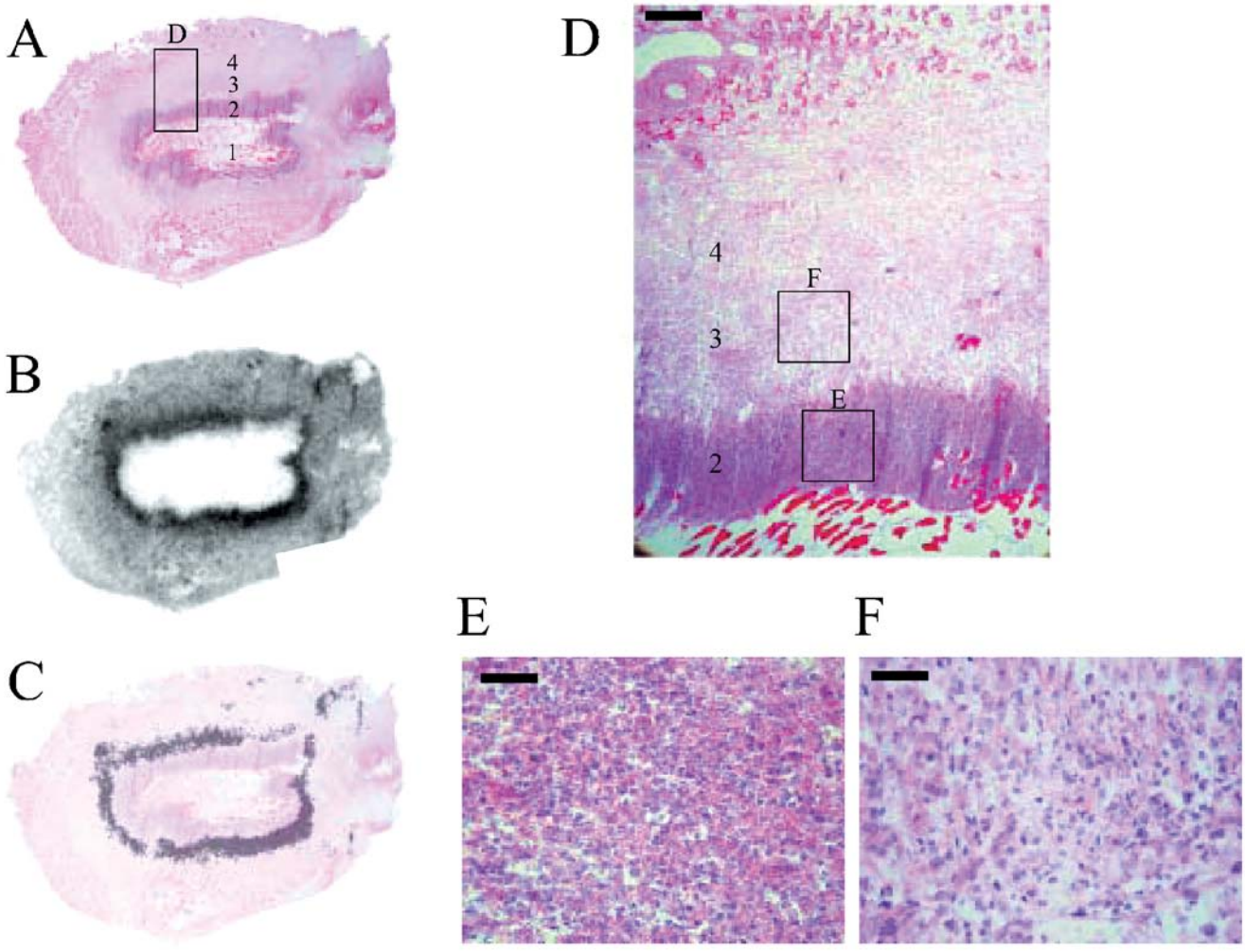

Fig. 1A–F. Histology of the abscess formation on day 7 (H-E staining, **A**), FCH autoradiography of the identical slice (**B**) and superposition of the two (**C**). The abscess wall (**D**) is characterised by a necrotic centre (*1*), which is surrounded by a layer consisting mainly of necrotic granulocytes (*2*; for higher magnification see **E**). Adjacent is a zone with granulation tissue, which can be subdivided into a more active inner (*3*, for higher magnification see **F**) and a more mature outer part (*4*). The highest concentration of FCH is found in layer 3, while layer 2 does not take up any FCH. Further details are reported in the text. The *bar* represents 400 µm in **D** and 100 µm in **E** and **F**

Table 2. SUV of tracer uptake determined with PET

Animal	FCH PET, day 6			FDG PET, day 5		
	Abscess	Normal ipsilateral	Muscle contralateral	Abscess	Normal ipsilateral	Muscle contralateral
1				4.12	1.72	2.10
2	1.06	0.45	0.30	4.53	0.95	0.55
3	1.17	0.38	0.28	2.36	0.86	0.42
4				2.36	0.81	0.44
5	1.13	0.35	0.29	3.45	1.29	0.63
Mean	1.12	0.39	0.29	3.37	1.13	0.83
SD	0.06	0.05	0.01	0.99	0.38	0.72

two animals examined 11 days following induction of the abscess, the mean SUV in layer 3 was 2.99 and 4.05 respectively. The corresponding values for layer 4 were 2.09 and 2.89 and for healthy muscle, 0.99 and 0.64.

FCH and FDG PET

The SUVs of tracer uptake determined with FCH and FDG PET are demonstrated in Table 2. In animals 1 and

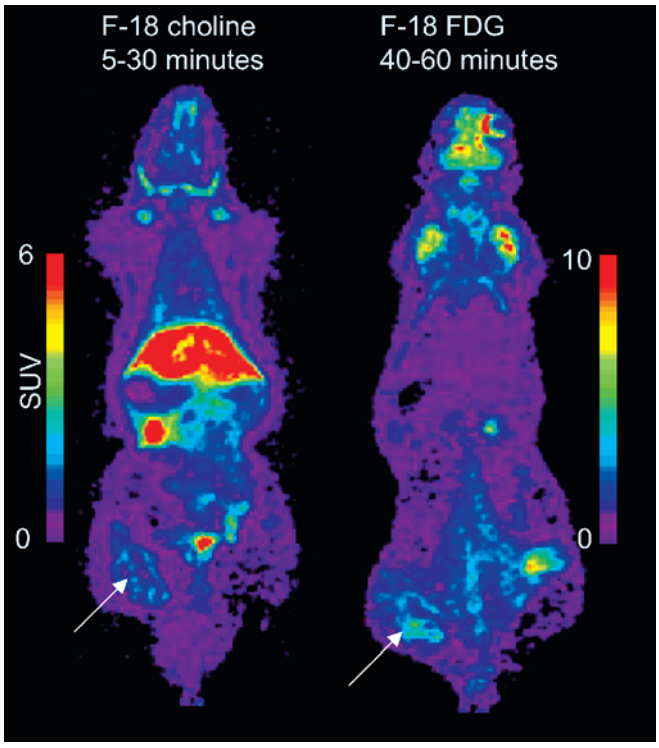

Fig. 2. FCH and FDG PET. Shown is a slice with a thickness and pixel size of 0.5 mm. The abscess (*arrows*) is clearly visualised with FCH (on the *left*) and FDG (on the *right*). With FCH the highest uptake is in the liver and kidney

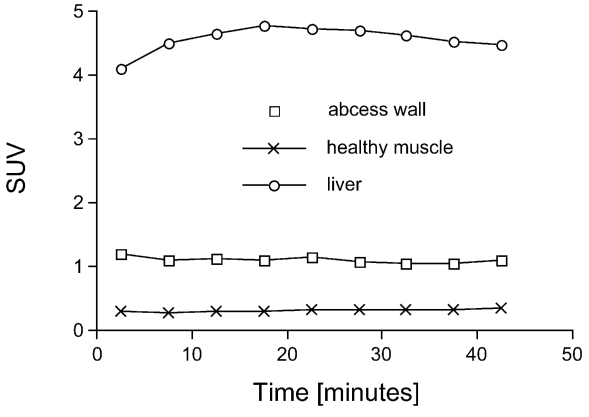

Fig. 3. Time course of the FCH concentration in different structures (mean of three animals)

4, tracer uptake was sluggish owing to partial paravenous injection of FCH. SUV values were therefore not calculated. In the other three animals the mean SUV in the abscess wall was 2.8 and 3.9 times higher than in ipsilateral and contralateral normal muscle respectively. With FDG, the abscess wall accumulated three to four times more tracer than normal muscle.

A slice of an FCH and an FDG PET scan are shown in Fig. 2. The abscess wall is clearly delineated with both tracers. With FCH the highest uptake is present in the liver and kidney. The time course of FCH concentration is illustrated in Fig. 3. In the abscess wall and in muscle tissue there was only minimal change between 5 and 45 min following injection. In the liver a maximum SUV of 4.75 was reached after 15–20 min.

Discussion

The most important result of this study is the demonstration of avid FCH uptake in inflammatory lesions. Such uptake will potentially limit the specificity of FCH in tumour evaluations. In the abscess wall the autoradiographically measured FCH SUV was 3 and 4 at days 7 and 11 respectively. This is somewhat lower than the FDG SUV determined with the same methods in one of our earlier experiments [12]. In that study the FDG SUV in the abscess wall was 5 and 8 at days 5 and 9 respectively. However, the important issue is how FCH SUV in infectious lesions compares with FCH uptake in tumours. In a study by Price et al. in patients with prostate cancer, the FCH SUV was between 2 and 8 in the prostate gland and between 3 and 8 in metastatic lymph nodes and bone metastasis [10]. Zhang et al. assessed the usefulness of ^{11}C-choline in separating benign from malignant lesions in bone and soft tissue tumours in 43 patients [13]. The SUV was 4.9±2.1 and 2.5±1.7 in malignant and benign lesions respectively. The data of both studies demonstrate that the SUV in certain tumorous lesions is in the same range as the SUV in the infectious tissue of our study (range 3–4).

Correlation of the FCH autoradiographs with the histology clearly demonstrated that the highest FCH uptake is found in the active granulation tissue (layer 3). The resolution of autoradiography does not allow identification of which cell types within this area incorporate FCH. However, since the main difference between the inner and the outer layer of the granulation tissue is the number of inflammatory cells, it seems likely that these cells accumulate a major part of the FCH. On day 11, FCH uptake in layers 3 and 4 is even higher than on day 7, with granulocytes no longer present. This suggests that a major part of the FCH is incorporated in macrophages at that stage, pointing to an upregulation of choline kinase in these cells, as has been demonstrated for tumour cells. Choline is transported into cells by specific mechanisms and then phosphorylated by choline kinase. In a further step it is metabolised to phosphatidylcholine and incorporated into the cell membrane. The increased choline uptake in tumours is explained by upregulation of choline kinase.

It is interesting that the layer with the highest cell density (layer 2) does not take up any FCH. This may be because this layer contains only dead cells or because it is not perfused, or a combination of the two. Another question is to what degree the observed FCH uptake pattern is determined by blood flow, which may vary in the different layers of the abscess wall.

The abscesses were clearly delineated by FCH and FDG PET. The contrast relative to surrounding tissue seemed similar for both tracers. Comparison of the SUVs determined with PET and autoradiography demonstrated an underestimation of the FCH SUVs by PET. This is most probably due to the limited spatial resolution of PET and the resultant underestimation of radioactivity concentration in small structures. Another factor may be the lack of attenuation correction, which is not implemented on the present system. Also the FDG SUVs in the abscess wall at day 5 were somewhat lower than the autoradiographically determined values in our previous study (3.3 vs 5 in the previous study [12]).

In summary, FCH is avidly accumulated in inflammatory infiltrates. This finding limits the specificity of labelled choline compounds for tumour detection. Future studies are now required to determine the degree of this limitation in human cancer patients. This includes the evaluation of FCH uptake in different acute and chronic inflammatory lesions.

Acknowledgements. The authors would like to thank Claudia Keller for the help with the data acquisition and Tibor Cservenjak for the radiotracer synthesis. This project was supported by the Wilhelm Sander Foundation.

References

1. Kaim AH, Weber B, Kurrer MO, Westera G, Schweitzer A, Gottschalk J, von Schulthess GK, Buck A. ^{18}F-FDG and ^{18}F-FET uptake in experimental soft tissue infection. *Eur J Nucl Med Mol Imaging* 2002; 29:648–654.
2. Weber WA, Wester HJ, Grosu AL, Herz M, Dzewas B, Feldmann HJ, Molls M, Stocklin G, Schwaiger M. *O*-(2-[^{18}F]fluoroethyl)-L-tyrosine and L-[methyl-^{11}C]methionine uptake in brain tumours: initial results of a comparative study. *Eur J Nucl Med* 2000; 27:542–549.
3. Hustinx R, Lemaire C, Jerusalem G, Moreau P, Cataldo D, Duysinx B, Aerts J, Fassotte MF, Foidart J, Luxen A. Whole-body tumor imaging using PET and 2-^{18}F-fluoro-L-tyrosine: preliminary evaluation and comparison with ^{18}F-FDG. *J Nucl Med* 2003; 44:533–539.
4. Hara T, Kosaka N, Kishi H. PET imaging of prostate cancer using carbon-11-choline. *J Nucl Med* 1998; 39:990–995.
5. de Jong IJ, Pruim J, Elsinga PH, Vaalburg W, Mensink HJ. Preoperative staging of pelvic lymph nodes in prostate cancer by ^{11}C-choline PET. *J Nucl Med* 2003; 44:331–335.
6. de Jong IJ, Pruim J, Elsinga PH, Vaalburg W, Mensink HJ, Visualization of prostate cancer with ^{11}C-choline positron emission tomography. *Eur Urol* 2002; 42:18–23.
7. DeGrado TR, Baldwin SW, Wang S, Orr MD, Liao RP, Friedman HS, Reiman R, Price DT, Coleman RE. Synthesis and evaluation of (18)F-labeled choline analogs as oncologic PET tracers. *J Nucl Med* 2001; 42:1805–1814.
8. DeGrado TR, Coleman RE, Wang S, Baldwin SW, Orr MD, Robertson CN, Polascik TJ, Price DT. Synthesis and evaluation of ^{18}F-labeled choline as an oncologic tracer for positron emission tomography: initial findings in prostate cancer. *Cancer Res* 2001; 61:110–117.
9. DeGrado TR, Reiman RE, Price DT, Wang S, Coleman RE. Pharmacokinetics and radiation dosimetry of ^{18}F-fluorocholine. *J Nucl Med* 2002; 43:92–96.
10. Price DT, Coleman RE, Liao RP, Robertson CN, Polascik TJ, DeGrado TR. Comparison of [^{18}F]fluorocholine and [^{18}F]fluorodeoxyglucose for positron emission tomography of androgen dependent and androgen independent prostate cancer. *J Urol* 2002; 168:273–280.
11. Mikolajczyk K, Szabatin M, Rudnicki P, Grodzki M, Burger C. A JAVA environment for medical image data analysis: initial application for brain PET quantitation. *Med Inform (Lond)* 1998; 23:207–214.
12. Kaim AH, Weber B, Kurrer M, Gottschalk J, von Schulthess GK, Buck A. Autoradiographic quantification of ^{18}F-FDG uptake in experimental soft tissue abscesses in rats. *Radiology* 2002; 223:446–451.
13. Zhang H, Tian M, Oriuchi N, Higuchi T, Watanabe H, Aoki J, Tanada S, Endo K. ^{11}C-choline PET for the detection of bone and soft tissue tumours in comparison with FDG PET. *Nucl Med Commun* 2003; 24:273–279.